A penalized nonparametric method for nonlinear constrained optimization based on noisy data.

Ronaldo Dias *, Nancy L. Garcia, Adriano Z. Zambom
Universidade Estadual de Campinas (UNICAMP)

Abstract

The objective of this study is to find a smooth function joining two points A and B with minimum length constrained to avoid fixed subsets. A penalized nonparametric method of finding the best path is proposed. The method is generalized to the situation where stochastic measurement errors are present. In this case, the proposed estimator is consistent, in the sense that as the number of observations increases the stochastic trajectory converges to the deterministic one. Two applications are immediate, searching the optimal path for an autonomous vehicle while avoiding all fixed obstacles between two points and flight planning to avoid threat or turbulence zones.

Key words: Autonomous vehicle, B-splines, consistent estimator, confidence ellipses, constrained optimization, nonparametric method.

1 Introduction

Finding the shortest path between two points in the presence of obstacles is an important problem in robotics, geographical information systems and in-flight planning

*Corresponding author: Ronaldo Dias – Departamento de Estatística, IMECC/UNICAMP – Caixa Postal 6065, 13.081-970 - Campinas, SP - BRAZIL, e-mail addresses: `dias@ime.unicamp.br`, `nancy@ime.unicamp.br`, `adrzzz@yahoo.com`

of routes. A classical application in robotics is the search for optimal trajectories for an autonomous vehicle which has to move from point A to point B traveling the minimum possible distance while avoiding all fixed obstacles between these points. A similar problem is to find a flight planning that avoids threat or turbulence zones. This avoidance must be achieved respecting some further constraints. For instance, a safe distance r must be kept at all times between the vehicle and the obstacles, while avoiding further areas like craters. Moreover, the trajectory has to follow a smooth curve because vehicles or planes cannot make abrupt turns. For more details about autonomous vehicles see information about DARPA Grand Challenge (http://www.darpa.mil/grandchallenge).

A large body of literature has emerged over the past two decades on motion planning for car-like mobile robots and Unmanned Aerial Vehicles (UAV). See the books [13, 19, 6] for introductory material, and [14, 15] for up-to-date results. Many deterministic approaches have been proposed for obstacle avoidance problems. They can be classified into search-based methods, geometric approaches, control theoretical methods and artificial potential field methods. Some authors use an exhaustive search-based method that explores the configuration space by propagating step motions for some controls, see for example [4]. The usual approach using dynamic programming divides the state space into cells of specified dimensions and places the restrictions in each cell along prescribed headings. The computational cost of this approach increases as the cell sizes decrease and the number of allowed headings increases. Moreover, the paths must be smoothed out to avoid abrupt heading changes. When the threat zones are circular, the simplest solution for the problem consists of straight line segments and circular arcs. The possible segments are easily enumerated by a search algorithm. Asseo [2] proposed an algorithm based on a geometric construction that uses linear segments tangent to the threat periphery and circular segments along the threat periphery, to obtain the shortest route between the starting and the destination points using the principle of optimality. This proposal cannot be generalized to non-circular threat zones. Graph theory has been used lately to construct planar coverage strategies for autonomous vehicle, see for instance [23].

Optimization problems posed by paths connecting two points have intrinsic mathematical interest and appear in a number of applications besides robotics. We mention, in particular, the *mountain-pass* problem, of importance in non-linear analysis and computational chemistry, which has been the object of a vast literature. See [16] for a good introduction to the subject. This problem, however, looks only to critical points of a path, rather than to the determination of the whole path.

We propose a penalized optimization procedure to obtain an approximate solution to the problem. We consider functions belonging to a finite-dimensional approximating space generated by a basis of B-splines and impose a penalization on solutions that do not comply with the constrains. Our approach presents several advantages: (i) It transforms an infinite-dimensional problem into a finite-dimensional one and, in practice, only few coefficients have to be computed; (ii) it naturally changes the constrained optimization into an unconstrained one, and (iii) it can easily deal with pop-up threats without increasing the run-time. However, perhaps the main novelty of our approach is that it can incorporate non-homogeneous error measurements in the location of the obstacles/threat zones, in which case it yields a consistent stochastic path. That is, it can treat situations in which the avoidance set is not known exactly but it is observed through a random mechanism that adds a random noise. In these cases it produces a stochastic solution that converges to the deterministic one as the number of independent observations increases.

In this paper, we will analyze the problem both under the deterministic and stochastic scenarios. The former is studied In Section 2. There we assume a vehicle/plane with perfect sensors that can find the obstacles/threat zones without error. In this case, the path planning is obtained by solving a penalized optimization problem. In Section 3 we consider noisy determination of obstacles and find a stochastic solution based on independent readings. This solution converges, as the number of readings increase, to the former deterministic solution. Furthermore, in Section 5 we consider briefly the stepwise case where $[0, b]$ is split into s pieces and the problem has to be solved sequentially in each sub-interval. This corresponds to an obstacle field that is not entirely known and a vehicle that cannot see the whole space. It also applies to situations with pop-up threat zones. This partial vision case is important not only *per se* but also because it allows to construct trajectories that are not graphs of functions. In this case, the trajectory is constructed piecewisely using the same algorithm. Similar ideas were used in practice during the 2005 DARPA Challenge by Caltech Team, see [7].

2 An optimization problem

In this work, we study the following nonlinear constrained optimization problem. Let $A = (x_a, y_a)$ and $B = (x_b, y_b)$ be two points in $\mathbb{R}^2$, with $x_a < x_b$. Without loss of generality, we will consider the can consider $A = (0, 0)$ and $B = (b, 0)$ (if not, a change of coordinates will accomplish the change). We search for a path with minimum length that can be represented as the graph of a smooth function f

$$\text{Graph}\,(f) \;=\; \{(x, y); x \in [x_a, x_b] \text{ and } y = f(x)\}.$$

To be precise on what we called a smooth trajectory, we consider only functions f belonging to a subset of the Sobolev space

$$\mathcal{H}_2^2 := \{f : [x_a, x_b] \to \mathbb{R}, \int f^2 < \infty, \int (f')^2 < \infty \text{and} \int (f'')^2 < \infty, f(x_a) = y_a, f(x_b) = y_b\}.$$

This Sobolev space is convenient for our purposes because it consists of smooth functions that can be well approximated by uniform B-splines, see [21]. Moreover, we want to constrain the search to paths that comply with the restriction of avoiding an open region $\Gamma \subset \mathbb{R}^2$ which represents a region around certain obstacles or threat zones. We need open regions in order to have a unique solution for the optimization problem (see explanation after (2.5)).

Therefore, the goal is to find a smooth function f belonging to $\mathcal{H}_K$ satisfying:

1. The trajectory has to go through the points $A = (0,0)$ and $B = (b,0)$, i.e. $f(0) = 0$ and $f(b) = 0$.
2. The trajectory has to avoid some set Γ around the obstacles (or the threat zones), that is, $\mathrm{Graph}\,(f) \cap \Gamma = \emptyset$ for some fixed open set Γ.
3. The function f minimizes the trajectory in the sense that the length of Graph (f) defined by
$$Q(f) := \int_0^b \sqrt{(1 + f'(t)^2)}dt$$
is minimum.

Notice that the constrained minimization problem can be viewed as a penalized problem where the penalty is 0 or ∞ according to $\mathrm{Graph}\,(f) \cap \Gamma = \emptyset$ (the path does not intercept the obstacle region) or not. That is, we want a solution of

$$\min_{f \in \mathcal{H}_2^2} \int_0^b \sqrt{(1 + f'(t))^2}dt + J^*(f) \tag{2.1}$$

where

$$J^*(f) = \begin{cases} 0, & \text{if } \mathrm{Graph}\,(f) \cap \Gamma = \emptyset, \\ \infty, & \text{if } \mathrm{Graph}\,(f) \cap \Gamma \neq \emptyset. \end{cases} \tag{2.2}$$

In general, to find the solution for (2.1) is very difficult or even, in some cases, does not exist depending on the set Γ, since we are restricting ourselves to functions belonging to $\mathcal{H}_2^2$.

For the sake of simplicity, from now on we will consider that we have L points in $\mathbb{R}^2$ with coordinates $\xi_i = (w_i, v_i), \quad i = 1, \ldots, L$. Denote by $N = \{\xi_1, \xi_2, \ldots, \xi_L\}$ and

$$\Gamma = \cup_{i=1}^L B(\xi_i, r)$$

where $B(\xi, r) = \{z \in \mathbb{R}^2; d(z, \xi) < r\}$ and d is the Euclidean distance. It is easy to see this set up can be generalized in a straightforward manner.

To overcome this problem, first we approximate the penalization by the smooth functional

$$J_{\psi,\alpha,n}(f) = \psi\Phi(Z_\alpha + \sqrt{H}(r - d(f,N))) \tag{2.3}$$

where $d(f,N) = \inf\{d(z,\xi); z \in \text{Graph}\,(f), \xi \in N\}$, Φ is the cumulative standard Gaussian distribution, Z_α is its αth percentile and (ψ,α,H) are tuning parameters. This penalization is convenient since it follows that $J_{\psi,\alpha,H}(f) \to J^*(f)$ when $\psi \to \infty$, $\alpha \to 0$ and $H \to \infty$. In Section 2.1 we explain the roles of the tuning parameters.

Second, it is well-known that $\mathcal{H}_2^2$ is an infinite-dimensional space, but it can be well approximated by a a finite dimensional space which is spanned by K (fixed) basis functions ([21]), such as Fourier expansion, wavelets, B-splines, natural splines, see for example [22], [18], [24], [10] and [12]. In this work, following [21] we will fix K and a sequence $\mathbf{t} = (t_1, \ldots, t_{K-2})$ and consider f belonging to the space $\mathcal{H}_K$ spanned by B-splines with interior knot sequence $\mathbf{t}$. That is,

$$f(x) \;=\; f_{\boldsymbol{\theta}}(x) \;=\; \sum_{j=1}^{K} \theta_j B_j(x) \tag{2.4}$$

where B_j are the well-known cubic B-spline basis (order 4) and $\boldsymbol{\theta} = (\theta_1, \ldots, \theta_K)$ is a vector of unknown coefficients.

Figure 2.1 presents 6 B-splines functions for equally spaced knots in the intervals $[0,1]$. From the picture we can see some of the most useful computational properties presented by B-splines. They are splines which have smallest possible support. In other words, B-splines are zero in a large set. Furthermore, a stable evaluation of B-splines with the aid of a recurrence relation is possible. For details, see [8].

Therefore, we want to find $f_{\boldsymbol{\theta}} \in \mathcal{H}_K$, or equivalently $\boldsymbol{\theta} = (\theta_1, \ldots, \theta_K) \in \mathbb{R}^K$ which minimizes

$$Q_{\alpha,\psi,r,H}(\boldsymbol{\theta}) = \int_0^b \left(1 + (\sum_{j=1}^{K} \theta_j B_j'(t))^2\right)^{1/2} dt + \psi\,\Phi\left(Z_\alpha + \sqrt{H}(r - d(\sum_{j=1}^{K} \theta_j B_j(\cdot), N))\right), \tag{2.5}$$

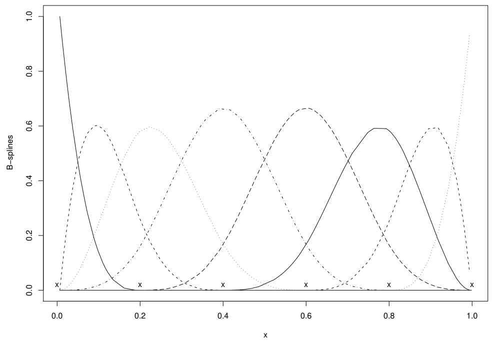

Figure 2.1: Basis Functions with 6 knots placed at $\mathbf{t} = (0.0, 0.2, 0.4, 0.6, 0.8, 1.0)$

subject to $f_{\boldsymbol{\theta}}(0) = 0, f_{\boldsymbol{\theta}}(b) = 0$. At this point we can see the need to consider only open balls around the obstacles (in general, Γ to be an open set), if not the minimum in (2.5) is not attainable.

Notice that the penalized approach is very appealing since it allows us to change the constrained nonlinear problem of finding a function into an unconstrained non-linear problem of finding a vector on $\mathbb{R}^{k-2}$. This problem was solved by using the function *fminunc* from MATLAB which is based on the well-known BFGS Quasi-Newton method with a mixed quadratic and cubic line search procedure.

2.1 The tuning parameters

Notice that the functionals J^* and $J_{\psi,\alpha,H}$ depend on the function f only through its distance to the obstacle field ($d(f, N)$), thus with an abuse of notation we introduce the real-valued functions defined for $x \in [0, \infty)$ as

$$J^*(x) = \begin{cases} 0, & \text{if } x \geq r, \\ \infty, & \text{if } x < r. \end{cases} \tag{2.6}$$

and

$$J_{\psi,\alpha,n}(x) = \psi\Phi(Z_\alpha + \sqrt{H}(r - x)). \tag{2.7}$$

The function $J_{\psi,\alpha,H}$ is a continuous analog of J^*. The roles of the tuning parameters (ψ, α, H) are $\psi\alpha = J_{\psi,\alpha,H}(r)$, $\psi = \max_{x\geq 0} J_{\psi,\alpha,H}(x)$ and H controls the steepness of $J_{\psi,\alpha,H}$ at the point r. They should be chosen in such way that, when the trajectory tries to violate the constraint (e.g, the distance between the vehicle and the obstacles have to be bigger than r at all times, the plane has to avoid threat zones) the penalization is so much bigger than the gain in the distance that this trajectory cannot occur. Figure 2.2 shows the effect of the tuning parameter H on the penalty $J_{\psi,\alpha,H}(f)$, for a better visualization we fixed $\psi\alpha = 30$. However, for computation and numerical examples we will use $\alpha.\psi = 0.05$.

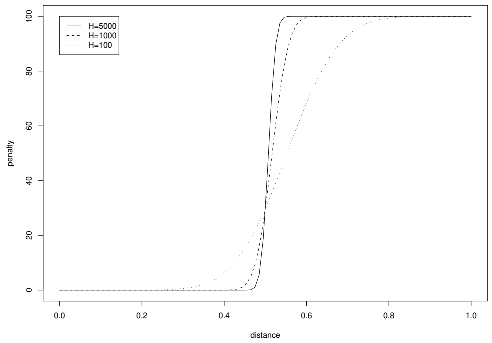

Figure 2.2: Effect of the tuning parameter H on the penalty function $J_{\psi,\alpha,H}(f)$, $\psi = 100$, $\alpha = 0.3$, $r = 0.5$.

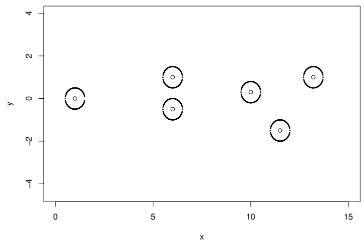

Figure 2.3: Example of a Γ set.

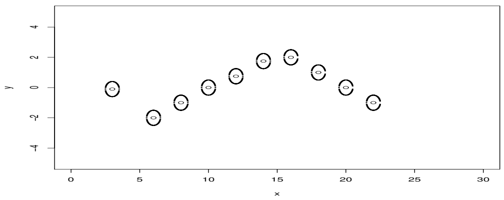

Figure 2.4: Example of a Γ set.

Tables 2.1 and 2.2 present some simulation results for Γ sets given by Figures 2.3 and 2.4. Notice that as ψ increases (α decreases, recall that $\psi = 0.05/\alpha$) and/or H

$3\alpha * 10^5$	10^{-3}	10^{-2}	10^{-1}	1
$n * 10^{-3}$				
.5	15.1311	15.1311	15.1311	15.1311
1.5	15.1286	15.1288	15.1290	15.1311
15	15.1241	15.1247	15.1248	15.1248
150	15.1237	15.1238	15.1238	15.1241
1500	15.1220	15.1220	15.1220	15.1221
15000	15.1211	15.1211	15.1211	15.1211

Table 2.1: Length of the chosen trajectory for Γ presented in Figure 2.3 .

$6\alpha * 10^5$	10^{-3}	10^{-2}	10^{-1}	1
$n * 10^{-3}$				
.5	30.0794	30.0794	30.0794	30.0794
3	30.0794	30.0794	30.0794	30.0794
30	30.0766	30.0776	30.0777	30.0778
300	30.0778	30.0778	30.0778	30.0778
3000	30.0757	30.0757	30.0758	30.0758
30000	30.0756	30.0756	30.0756	30.0757

Table 2.2: Length of the chosen trajectory for Γ presented in Figure 2.4.

increases we get closer and closer to the best trajectory until it stabilizes. From these simulated results, we choose $\psi = 10^6 b$, $\alpha = 0.05/\psi$ e $H = 10^6 b$.

How many knots? In fact, in approximation theory, one of the most challenging problem is how to select the dimension of the approximant space. A similar problem is encountered in the field of image processing where the level of resolution needs to be determined appropriately. Figure 2.5 presents several Γ sets with different degrees of difficulty for finding a trajectory. These fields were construct to test the strength of the algorithm since the best route is not "easy". We could see that increasing the number of interior knots above 4 did not bring any improvement. With 3 or 4 interior knots we obtain the "best" possible $f_{\boldsymbol{\theta}}$. If necessary, the choice of the number of knots can be very adaptive, see for example [11], [20], [1] [9], [5], [17] and easily implemented.

3 A stochastic problem. Complete Vision

In the previous section, we assumed that the Γ set is deterministic, in the applications this would mean the sensors of the vehicle/plane can see the whole field and detect with certainty the placement of the obstacles/threat zones. This is not realistic, there is always a measurement error involved. In this section, we will suppose that the sensors can see the whole field (partial vision will be considered in Section 5) but instead of seeing N, they see $\eta = N + \boldsymbol{\varepsilon}$ where $\boldsymbol{\varepsilon} = (\varepsilon_1, \ldots, \varepsilon_L)$ is the measurement error. Specifically, we will assume that

$$\Gamma = \cup_{\ell=1}^{L} B((w_\ell, v_\ell), r)$$

but the observations are given by $(W_\ell, V_\ell) = (w_\ell, v_\ell) + (\varepsilon_{\ell 1}, \varepsilon_{\ell 2})$, $\quad \ell = 1, ..., L$, with $(\varepsilon_{\ell 1}, \varepsilon_{\ell 2}) \sim N_2((0,0), \boldsymbol{\Sigma}_i)$, $\ell = 1, \ldots, L$ independent random variables with covariance

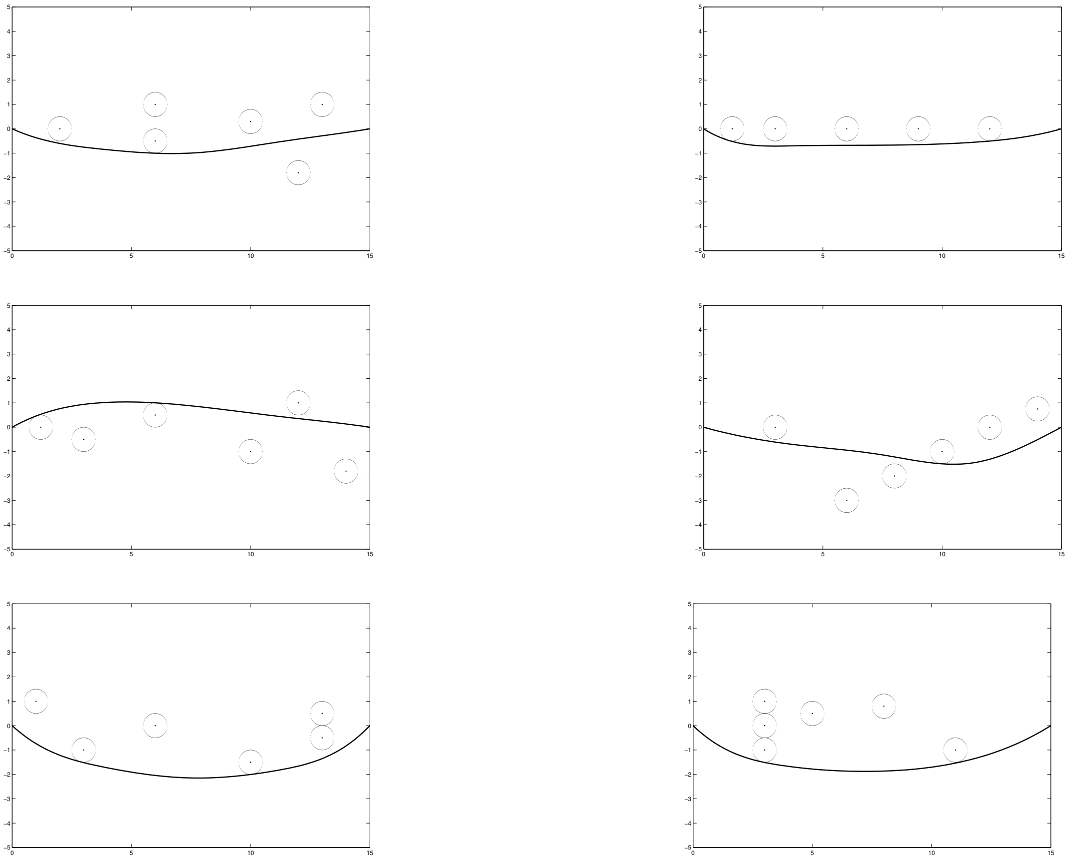

Figure 2.5: Estimated "best" trajectory using 4 internal knots

structure given by $\boldsymbol{\Sigma}_\ell$ (that can depend on the point (w_ℓ, v_ℓ)) given by

$$\boldsymbol{\Sigma}_\ell = \begin{pmatrix} \sigma_{\ell,1}^2 & \rho\sigma_{\ell,1}\sigma_{\ell,2} \\ \rho\sigma_{\ell,1}\sigma_{\ell,2} & \sigma_{\ell,2}^2 \end{pmatrix}. \tag{3.1}$$

This scenario incorporates several practical situations, for example larger variance for darker spots, increasing variance depending on the distance to the obstacle/threat zone, easier to spot threat zones, etc.

Moreover, we have for each point, n independent readings. Thus, our data is composed of n readings of the point process $\eta_i = \{(W_{1,i}, V_{1,i}), \ldots, (W_{L,i}, V_{L,i})\}$ for $i = 1, \ldots, n$. Denote $\mathbf{W}_\ell = (W_{\ell,1}, \ldots, W_{\ell,n})$ and $\mathbf{V}_\ell = (V_{\ell,1}, \ldots, V_{\ell,n})$, $\ell = 1, \ldots, L$.

For a sequence $\gamma_n \in (0,1)$, the proposed estimator for $f_{\boldsymbol{\theta}}$ is the function

$$f_{\hat{\boldsymbol{\theta}}_n}^{\gamma_n}(x) \;=\; \sum_{j=1}^{K} \hat{\theta}_j B_j(x) \tag{3.2}$$

where $\hat{\boldsymbol{\theta}}_n$ is the solution of the minimization problem

$$\hat{\boldsymbol{\theta}}_n \;=\; \arg\min Q_{\alpha,\psi,r,H,n}(\boldsymbol{\theta}) \tag{3.3}$$

subject to $f_{\boldsymbol{\theta}}^{\gamma}(0) = 0, f_{\boldsymbol{\theta}}^{\gamma}(b) = 0$, where

$$Q_{\alpha,\psi,r,H,n}(\boldsymbol{\theta}) = \int_0^b \left(1 + (\sum_{j=1}^{K} \theta_j B_j'(t))^2\right)^{1/2} dt + \psi\, \Phi\left(Z_\alpha + \sqrt{H}(r - d(\sum_{j=1}^{K} \theta_j B_j(\cdot), \Gamma_n^{\gamma_n}))\right), \tag{3.4}$$

(*cf.* with Equation (2.5)). The set $\Gamma_n^{\gamma_n}$ is defined by

$$\Gamma_n^{\gamma_n} = \bigcup_{\ell=1}^{L} G^{\gamma_n}(\mathbf{W}_\ell, \mathbf{V}_\ell) \tag{3.5}$$

where for each $\ell = 1, \ldots, L$, $G^{\gamma_n}(\mathbf{W}_\ell, \mathbf{V}_\ell)$ is a $100(1-\gamma_n)\%$ *confidence ellipse* based on the n readings for the ℓth point $(\mathbf{W}_\ell, \mathbf{V}_\ell)$ defined as the ellipse formed by the points (x, y) that satisfy the equation

$$n((\overline{\mathbf{W}}_\ell, \overline{\mathbf{V}}_\ell) - (x,y))^t \boldsymbol{\Sigma}_\ell^{-1}((\overline{\mathbf{W}}_\ell, \overline{\mathbf{V}}_\ell) - (x,y)) \leq \chi_2^2(\gamma_n)$$

where $\overline{\mathbf{W}}_\ell$ and $\overline{\mathbf{V}}_\ell$ are the sample average of the vectors $\mathbf{W}_\ell$ and $\mathbf{V}_\ell$ respectively, $\chi_2^2(\gamma_n)$ is the $100\gamma_n$-percentile of the chi-square distribution with 2 degrees of freedom. These ellipses are centered at the sample mean $(\overline{\mathbf{W}}_\ell, \overline{\mathbf{V}}_\ell)$ and have axes $(\sqrt{\chi_2^2(\gamma_n)\,\lambda_{\ell,j}/n}\, e_{\ell,j}, -\sqrt{\chi_2^2(\gamma_n)\,\lambda_{\ell,j}/n}\, e_{\ell,j})$, where $\lambda_{\ell,j}$, $j = 1, 2$ are the eigenvalues of $\mathbf{\Sigma}_\ell$ and $e_{\ell,j}$ are the corresponding eigenvectors.

Here, $\Gamma_n^{\gamma_n}$ can be thought as a fattening of the averaged point process $\bar{\eta} = \frac{1}{n}(\eta_1 + \ldots + \eta_n)$ to account for the variability due to measurement errors. The confidence limits $1-\gamma_n$ will be chosen suitably in order to get strong convergence of the estimators (Theorem 3.2).

Remark. If the covariance matrices $\mathbf{\Sigma}_\ell$ are unknown, the points (x, y) belonging to the confidence ellipses have to satisfy

$$n((\overline{\mathbf{W}}_\ell, \overline{\mathbf{V}}_\ell) - (x, y))^t \mathbf{S}_\ell^{-1}((\overline{\mathbf{W}}_\ell, \overline{\mathbf{V}}_\ell) - (x, y)) \leq \frac{2(n-1)}{(n-2)} F_{2,n-2}(\gamma_n)$$

where $\mathbf{S}_\ell$ is the standard sample covariance of the vectors $\mathbf{W}_\ell$ and $\mathbf{V}_\ell$ and $F_{2,n-2}(\gamma_n)$ is the $100\gamma_n$-percentile of the F distribution with $(2, n-2)$ degrees of freedom.

Lemma 3.1 *If* $\sum 1 - (1-\gamma_n)^L < \infty$ *then*

$$\mathbb{P}\,(N \notin \eta_n^{\gamma_n} \text{ i.o. }) \;=\; 0. \tag{3.6}$$

Proof. Since the processes $\eta_1, \ldots, \eta_L$ are independent, by the definition of confidence ellipses we have

$$\mathbb{P}\,(N \in \eta_n^{\gamma_n}) \;=\; \prod_{\ell=1}^{L} \mathbb{P}((w_\ell, v_\ell) \in G^{\gamma_n}(\mathbf{W}_\ell, \mathbf{V}_\ell)) \;=\; (1-\gamma_n)^L.$$

Thus, the result follows immediately from the Borel Cantelli Lemma. $\square$

Lemma 3.2 *(a)* $\{(\bar{W}_\ell, \bar{V}_\ell), \ell = 1, \ldots, L\} \to N,$ *a.s..*
(b) If $\chi_2^2(\gamma_n)/n \to 0$ *then* $\Gamma_n^{\gamma_n} \to N,$ *a.s. as* $n \to \infty$.
(c) For fixed $\theta \in \mathbb{R}^K$ *we have*

$$Q_{\alpha,\psi,r,H,n}(\theta) \to Q_{\alpha,\psi,r,H}(\theta), \quad a.s. \tag{3.7}$$

as $n \to \infty$.

Proof. (a) follows directly from the Strong Law of Large Numbers for i.i.d random vectors.

To prove (b) we just have to notice that the set $\Gamma_n^{\gamma_n}$ is the union of ellipses with centers at the points of N and axes having length $2\sqrt{\chi_2^2(\gamma_n)\,\lambda_{\ell,j}/n}$.

(c) is directly implied by (a) and (b). □

Notice that it is possible to satisfy simultaneously the conditions of Lemmas 3.1 and 3.2. By Chernoff inequality, for any random variable Z we have

$$\mathbb{P}(Z > a) \leq e^{-at}\mathbb{E}(e^{Zt}), \qquad \text{for all } t.$$

Thus taking $Z \sim \chi_2^2$ we obtain

$$\gamma_n \leq e^{-\chi_2^2(\gamma_n)t}\left(\frac{1}{1-2t}\right).$$

From now on, to simplify the notation we will drop the subscript (α, ψ, r, H).

Lemma 3.3 *For any continuous functions $f : [0, b] \to \mathbb{R}$ and $g : [0, b] \to \mathbb{R}$ and $\Gamma \subset \mathbb{R}^2$ we have*

$$\sup_{x\in[0,b]} |f(x) - g(x)| \geq |d(f, \Gamma) - d(g, \Gamma)|.$$

Proof. In fact, let $\epsilon = \sup_{x\in[0,b]} |f(x) - g(x)|$ and without loss of generality assume $d(f, \Gamma) > d(g, \Gamma)$. It is easy to see that for any $x \in [0, b]$ and $w \in \Gamma$

$$d((x, f(x)), w) \leq |f(x) - g(x)| + d((x, g(x)), w).$$

Therefore,

$$\begin{aligned} d((x, f(x)), \Gamma) &\leq |f(x) - g(x)| + d((x, g(x)), \Gamma) \\ &\leq \epsilon + d((x, g(x)), \Gamma) \end{aligned}$$

The result follows immediately by taking infimum over $x \in [0, b]$ in the last inequality.

□

Theorem 3.1 *The functions Q_n and Q are continuous functions.*

Proof. We just need to check that the map $\theta \mapsto \Phi\left(Z_\alpha + \sqrt{H}(r - d(\sum_{j=1}^K \phi_j B_j(\cdot), \Gamma))\right)$ is continuous for any set $\Gamma \subset \mathbb{R}^2$. In fact, this map is Lipschitz. To see this, take $\theta, \phi \in \mathbb{R}^K$

$$\begin{aligned}
&|\Phi\left(Z_\alpha + \sqrt{H}(r - d(\sum_{j=1}^K \theta_j B_j(\cdot), \Gamma))\right) - \Phi\left(Z_\alpha + \sqrt{H}(r - d(\sum_{j=1}^K \phi_j B_j(\cdot), \Gamma))\right)| \\
&\qquad = |\Phi'(\xi)\sqrt{H}\left(d(\sum_{j=1}^K \theta_j B_j(\cdot), \Gamma) - d(\sum_{j=1}^K \phi_j B_j(\cdot), \Gamma)\right)| \\
&\qquad \leq \frac{1}{\sqrt{2\pi}}\sqrt{H} \sup_{z\in[0,b]} |\sum_{j=1}^K (\theta_j - \phi_j) B_j(z)| \\
&\qquad \leq C|\theta - \phi|
\end{aligned}$$

for a suitable positive constant C. The equality follows from the Mean Value Theorem, for some $\xi \in \mathbb{R}$. The first inequality follows from Lemma 3.3 and $\Phi'(\xi) = (1/\sqrt{2\pi}) \exp(-\xi^2/2)$. □

To prove the main theorem, it is important to notice that Q_n is a random function since it depends upon the random processes $\eta_i = \{(W_{1,i}, V_{1,i}), \ldots, (W_{L,i}, V_{L,i})\}$ for $i = 1, \ldots, n$ through the confidence ellipse $\Gamma_n^{\gamma_n}$. In the following proof, when needed, we emphasize the fact that we are dealing with a specific realization ω writing $Q_n(\theta, \omega)$ and $\Gamma_n^{\gamma_n}(\omega)$.

Lemma 3.4 *For any $\phi \in \mathbb{R}^K$ we have*

$$\mathbb{P}\left(Q_n(\phi) < Q(\phi) \ i.o.\right) = 0 \tag{3.8}$$

Proof. From Lemma 3.1 we have that the event $A = [N \not\in \eta_n^{\gamma_n} \text{ i.o.}]$ has probability zero. This means that for any $\omega \in A^c$ there exists $n_0(\omega)$ with

$$N \subset \Gamma_n^{\gamma_n}(\omega)$$

for all $n \geq n_0$.

Therefore, for $\omega \in A^c$ and any $\phi \in \mathbb{R}^K$ we have

$$d(\sum_j \phi_j B_j, \Gamma_n^{\gamma_n}(\omega)) \leq d(\sum_j \phi_j B_j, N) \tag{3.9}$$

for all $n \geq n_0$. Thus, for any choice of the tuning parameters,

$$\psi\, \Phi \left(Z_\alpha + \sqrt{H}(r - d(\sum_{j=1}^{K} \phi_j B_j(\cdot), \Gamma_n^{\gamma_n})) \right) \geq \psi\, \Phi \left(Z_\alpha + \sqrt{H}(r - d(\sum_{j=1}^{K} \phi_j B_j(\cdot), N)) \right)$$

since Φ is strictly increasing, $\psi, H > 0$. Hence, for all $\omega \notin A$

$$Q_n(\phi, \omega) \geq Q(\phi), \tag{3.10}$$

for all $n \geq n_0$. Equation (3.8) follows immediately. □

We now can state the main theorem of this paper.

Theorem 3.2 *The solution of (3.3), $\hat{\boldsymbol{\theta}}_n$, is a strongly consistent estimator for $\boldsymbol{\theta}$, the solution of (2.5).*

Proof. In this case, we need the concept of *epiconvergence*. We need to prove that Q_n epiconverges to Q as $n \to \infty$. The following result is true: if θ_n is an ϵ_n minimizer of Q_n with $\epsilon_n \to 0$, then any convergent sub-sequence of $\{\theta_n\}$ must converge to a point θ which minimizes Q and the optimal value $Q_n(\theta_n)$ must also converge to the minimal point $Q(\theta)$. Notice that there is no need for uniqueness of the minimizers. If Q has a unique minimizer θ then θ is the only accumulation point of the sequence $\{\theta_n\}$. Also, it does not guarantee that θ is finite. There are several characterizations of epiconvergence, we follow [3]. The sequence Q_n epiconverges to Q if:

$$Q(\theta) \leq \sup_{B \in \mathcal{N}(\theta)} \liminf_{n \to \infty} \inf_{\phi \in B} \{Q_n(\phi)\}, \tag{3.11}$$

$$Q(\theta) \geq \sup_{B \in \mathcal{N}(\theta)} \limsup_{n \to \infty} \inf_{\phi \in B} \{Q_n(\phi)\} \tag{3.12}$$

where $\mathcal{N}(\theta)$ denotes the set of neighborhoods of the point θ.

Notice that there exists a countable base $\mathcal{B} = \{B_1, B_2, \ldots\}$ for the topology of $\mathbb{R}^K$. For any point θ, let

$$\mathcal{N}_c(\theta) \;=\; \mathcal{B} \cap \mathcal{N}(\theta).$$

Then, in our case, the suprema over uncountable set $\mathcal{N}(\theta)$ in (3.12) and (3.11) can be replaced by suprema over the countable set $\mathcal{N}_c(\theta)$.

First we will prove (3.12). If $B \in \mathcal{B}$ and $\theta \in B \in \mathcal{N}_c(\theta)$ then

$$Q(\theta) = \lim_{n\to\infty} Q_n(\theta) = \limsup{}_{m\to\infty} Q_m(\theta) \geq \limsup{}_{m\to\infty} \inf_{\phi\in B} Q_m(\phi)$$

since by Corollary 3.2

$$\Phi\left(Z_\alpha + \sqrt{H}(r - d(\sum_{j=1}^{K}\phi_j B_j(\cdot), \Gamma_n^{\gamma_n}))\right) \to \Phi\left(Z_\alpha + \sqrt{H}(r - d(\sum_{j=1}^{K}\phi_j B_j(\cdot), N))\right),$$

almost surely, as $n \to \infty$. Therefore,

$$Q(\theta) \geq \sup_{B\in\mathcal{N}_c(\theta)} \limsup{}_n \inf_{B\in B} Q_n(\phi).$$

and (3.12) is proved.

For (3.11), first we choose a countable dense set $\Theta_c = \{\theta_1, \theta_2, \ldots\}$ as follows. For each n, let $\theta_n \in B_n$ such that

$$Q(\theta_n) \leq \inf_{\phi\in B_n} Q_n(\phi) + \frac{1}{n}.$$

Therefore,

$$\begin{aligned}
\sup_{B_n\in\mathcal{N}_c} \liminf{}_{m\to\infty} \inf_{\phi\in B_n} Q_m(\phi) \;&\geq\; \sup_{B_n\in\mathcal{N}_c} \inf_{\phi\in B_n} Q(\phi) \\
&\geq\; \sup_{B_n\in\mathcal{N}_c} \left\{Q(\theta_n) - \frac{1}{n}\right\} \\
&\geq\; Q(\theta)
\end{aligned}$$

where the first inequality follows from Lemma 3.4. $\square$

4 Numerical examples for complete vision

In this section, we will use the language of the path finding for an autonomous vehicle. We performed numerical simulations for a large variety of obstacle fields. For illustration purposes, we exhibit only the cases where we have one and ten readings for each obstacle.

In all the plots the black points are the real obstacles, the crosses are mean of the observed obstacles, the confidence ellipses curves are drawn in gray. The solid curve is the curve we would obtain by the procedure described in Section 2 if we had no measurement error. The dashed and dash-point curves are the ones obtained by (3.3).

(a) 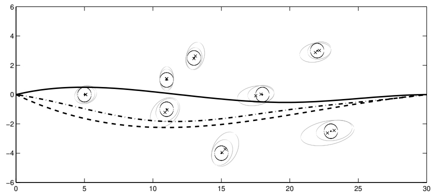 (b) 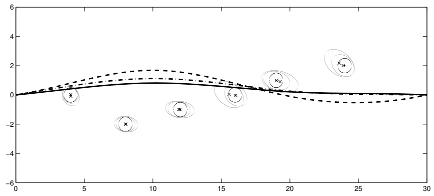

Figure 4.6: Estimated trajectories for independent case: deterministic trajectory (solid curve), trajectories based on one and ten observations (dashed line, dash-point line). The errors are normally distributed with (a) $\rho = 0.6$, $\sigma_{\ell,1} \sim U(0, (.8/30)W_\ell)$ and $\sigma_{\ell,2} \sim U(0, (.6/30)W_\ell)$, (b) $\rho = -0.7$, $\sigma_{\ell,1} \sim U(0, (.7/30)W_\ell)$ and $\sigma_{\ell,2} \sim U(0, (.5/30)W_\ell)$.

Figures 4.6 and 4.7 show that in the presence of random variability, the paths tend to stay further from the obstacle, but as the number of reading increases it will converge to the deterministic trajectory.

Figure 4.8 presents two examples where the obstacle field is highly structured and exhaustive search-based methods have to analyze several unfeasible trajectories. On the other hand, these type of obstacle fields do not pose any extra complexity or increase in the running time for our algorithm.

As pointed before, the procedure is not limited to avoiding circular sets. Figure

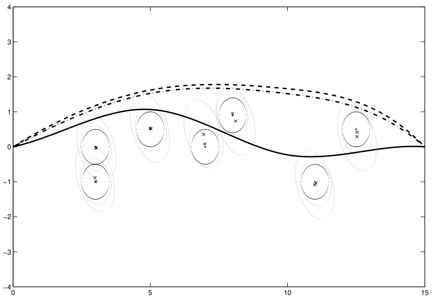

(a)

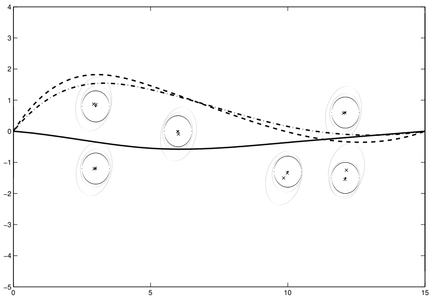

(b)

Figure 4.7: Estimated trajectories for iid case: deterministic trajectory (solid curve), trajectories based on one and ten observations (dashed line, dash-point line). The errors are normally distributed with (a) $\sigma_1 = 0.1$, $\sigma_2 = 0.2$ and $\rho = -0.8$ and (b) $\sigma_1 = 0.07$, $\sigma_2 = 0.15$ and $\rho = 0.6$.

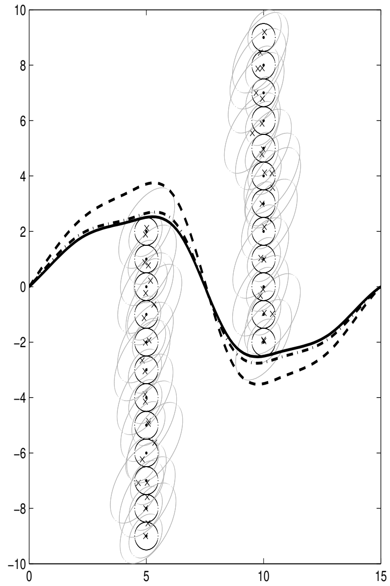

(a)

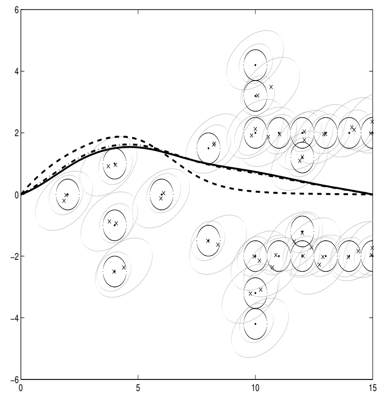

(b)

Figure 4.8: Estimated trajectories for iid case: deterministic trajectory (solid curve), trajectories based on one and ten observations (dashed line, dash-point line). The errors are normally distributed with (a) $\sigma_1 = 0.3$, $\sigma_2 = 0.4$ and $\rho = 0.8$ and (b) $\sigma_1 = 0.3$, $\sigma_2 = 0.2$ and $\rho = 0.7$.

4.9 (cf. Figure 4.7) presents the solution of the deterministic problem for diamond type sets.

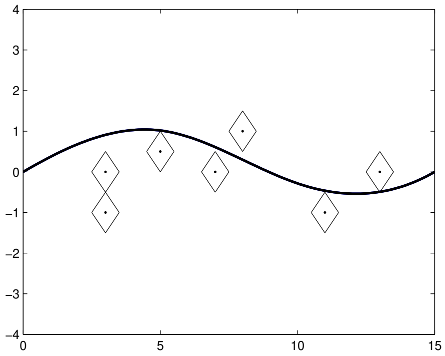

(a)

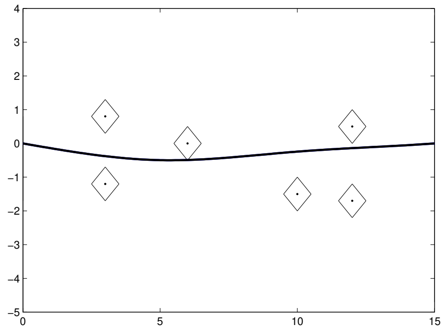

(b)

Figure 4.9: Estimated trajectories for deterministic trajectory for diamond obstacles

5 Partial vision

In the previous sections, we assumed that the whole point processes and consequently the set Γ is known in advance. Suppose, however, that we would like to construct the trajectory stepwisely at the points $0 < x_1 < x_2 < \ldots < x_N < b$ and at each "checkpoint" a new Γ is presented. In terms of the applications, maybe the obstacle field cannot be seen from the starting point and the strategy cannot be computed before leaving. In fact, it is more realistic to imagine that the sensors have a finite range R smaller than the total field. In this case, a sequential procedure is necessary.

For $(u, v) \in \mathbb{R}^2$ denote

$$S_{u,v} = \{(x, y) : 0 < x - u \leq R\}.$$

The proposed algorithm to estimate the best trajectory is:

1. Let N_1 be the point process N restricted to $S_{(0,0)}$. Let $\hat{f}_1 \in \mathcal{H}_K$ be the minimizer

of the cost function

$$\int_0^B \sqrt{1 + f_1'(t)^2} dt + \lambda\Phi(Z_\alpha + \sqrt{n}(r - d(f_1, N_1))) \tag{5.1}$$

where $f_1(0) = 0$, $f_1(b) = 0$.

2. Given the solution $\hat{f}_{i-1}$ at step $i - 1$, let N_i be the Point process N restricted to $S_{((i-1)R,0)}$. Let $\hat{f}_i \in \mathcal{H}_K$ be the minimizer of

$$\int_0^B \sqrt{1 + f_i'(t)^2} dt + \lambda\Phi(Z_\alpha + \sqrt{H}(r - d(f_i, N_i))), \tag{5.2}$$

subject to $f_i^{(\nu)}((i-1)R) = \hat{f}_{i-1}^{(\nu)}((i-1)R)$, for $\nu = 0, 1, 2$, $f_i(b) = 0$.

This sequential procedure can be interpreted as: the vehicle "thinks" at step i that there is no obstacles after distance R. When it arrives at checkpoints $R, 2R, \ldots$ it restarts the procedure joining smoothly the paths. Another important remark is that, at step i the procedure is not exactly as it was in the beginning because the vehicle will be at a point (iR, y_i), for some y_i not necessarily 0.

Notice that this estimation was described considering the deterministic case. The stochastic procedure can be easily implemented in this case.

(a) 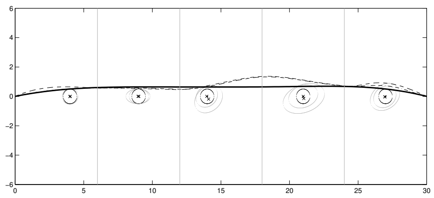 (b) 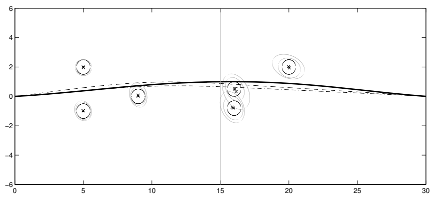

Figure 5.10: The solid curve is the goal path estimated using (2.5), the dashed and dash-point curves are sequentially estimated reloading stepwisely at the gray vertical lines. The errors are normally distributed with com (a) $\rho = 0.5$, $\sigma_{\ell,1} \sim U(0, (.6/30)W_\ell)$, $\sigma_{\ell,2} \sim U(0, (.4/30)W_\ell)$ and reload at steps of size 6 (b) $\rho = -.6$, $\sigma_{\ell,1} \sim U(0, (.5/30)W_\ell)$, $\sigma_{\ell,2} \sim U(0, (.6/30)W_\ell)$ and reload at steps of size 15.

Figure 5.10 show the simulated results for this case. Figure 5.10(b) raises a very important issue that is to be addressed in a future paper. Since the trajectory is computed at points $x_1, x_2, \ldots, x_N$, this can be interpreted as the vehicle only reloads after running the whole R distance. Since the path has to be smooth, if there is a point very close to the line x_i the vehicle when it gets there it will not deviate from the obstacle and crashes. To fix this problem, the vehicle should reload at shorter steps and the procedure redone. In this case, a very interesting scenario appears. Assume that the range of vision of the vehicle is R, it reloads after steps of size $R/2^\nu$ and the measurement errors are more precise as the distance between the sensors and the obstacles decrease, how to combine different readings, for example from point 0, point $R/2^\nu$, $R/2^{\nu-1}$, etc?

6 Conclusion

It is important to emphasize that the methodology presented in this paper can be generalized to the following more complex real situations.

1. *Dependent readings*

   For the case of partial vision, a more realistic assumption is that after each step of size $R/2^\nu$, the sensors make new readings from the obstacle field through procedures dependent on the previous readings. In the simplest case it would be a Markovian dependence.

   Suppose that at each step j of horizontal displacement of size $R/2^\nu$, the vehicle observes the point process $\eta_j = N_j + \boldsymbol{\varepsilon}_j$ with $\boldsymbol{\varepsilon}_j = (\varepsilon_{j,1}, \ldots, \varepsilon_{j,L}), j = 1, ..., [w_\ell 2^\gamma/R] + 1$ but the readings for the same obstacle ℓ, are dependent. If they have a joint normal distribution,

$$\begin{pmatrix} W_{\ell,j} \\ V_{\ell,j} \\ W_{\ell,j-1} \\ V_{\ell,j-1} \end{pmatrix} \sim N_4\left(\begin{pmatrix} \mu \\ \mu \end{pmatrix}, \begin{pmatrix} \Sigma_{\ell,j,j} & \Sigma_{\ell,j,j-1} \\ \Sigma_{\ell,j-1,j} & \Sigma_{\ell,j-1,j-1} \end{pmatrix}\right) \qquad (6.1)$$

for $j = 2, \ldots, L$, the distribution of $(W_{\ell,j}, V_{\ell,j})$ given $(W_{\ell,j-1}, V_{\ell,j-1}) = \mathbf{x}$ is normally distributed with mean

$$\Upsilon := \mu + \Sigma_{\ell,j,j-1}\Sigma^{-1}_{\ell,j-1,j-1}(\mathbf{x} - \mu)$$

and variance

$$\Xi := \Sigma_{\ell,j,j} - \Sigma_{\ell,j,j-1}\Sigma^{-1}_{\ell,j-1,j-1}\Sigma_{\ell,j-1,j}.$$

That is, at each reading the mean and the variance is corrected using the previous observation.

2. *Race corridors*

   Sometimes the vehicles or planes have to stay inside a prescribed area or road. Moreover, there could be checkpoints along the race. This can be seen, for example, in the DARPA Grand Challenge. See Figure 6.11.

The main advantage of our penalty approach is its flexibility to incorporate these new factors. Realistic complex problems can only be solved through decomposition into smaller and simpler pieces. This paper is a contribution to the analysis of the latter. We think that our adaptive obstacle avoidance strategies can be built efficiently into more sophisticated algorithms.

Acknowledgments We thank Richard Murray and Timothy Chung for introducing us to this problem and for many fruitful discussions. Also, Mario Martinez helped us discussing the problem. RD thanks the hospitality and enlightening environment provided by Caltech during his visit. We would like to thank the associate editor and the anonymous referee for valuable suggestions that greatly improved this paper. This paper was partially supported by CNPq Grants 301058/2004-0 (RD) and 302279/2004-0 (NG) and FAPESP Grant 2006/02095-5 (AZ).

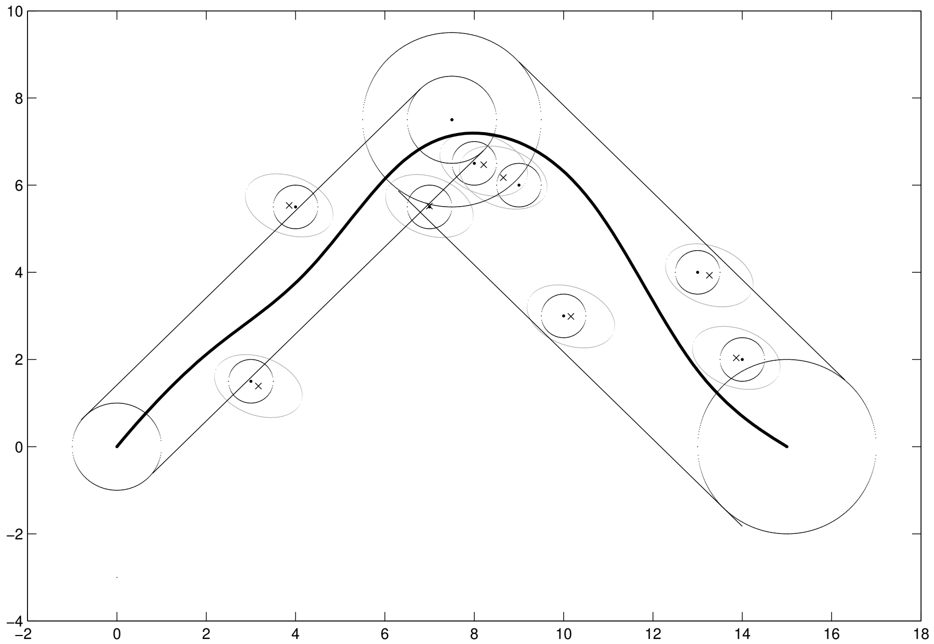

Figure 6.11: Trajectory constrained to avoid obstacles, to follow a road and to pass through one checkpoint at (8,7.5)

References

[1] Anestis Antoniadis. Wavelet methods for smoothing noisy data. In *Wavelets, images, and surface fitting (Chamonix-Mont-Blanc, 1993)*, pages 21–28. A K Peters, Wellesley, MA, 1994.

[2] S.J. Asseo. In-flight replanning of penetration routes to avoid threat zones of circular shapes. *Aerospace and Electronics Conference, 1998. NAECON 1998. Proceedings of the IEEE 1998 National*, pages 383–391, 1998.

[3] H. Attouch. *Variational convergence for functions and operators*. Applicable Mathematics Series. Pitman (Advanced Publishing Program), Boston, MA, 1984.

[4] Jérôme Barraquand and Jean-Claude Latombe. Nonholonomic multibody mobile robots: controllability and motion planning in the presence of obstacles. *Algorithmica*, 10(2-4):121–155, 1993. Computational robotics: the geometric theory of manipulation, planning, and control.

[5] Per Bodin, Lars F. Villemoes, and Bo Wahlberg. Selection of best orthonormal rational basis. *SIAM J. Control Optim.*, 38(4):995–1032 (electronic), 2000.

[6] H. Choset, K. Lynch, S. Hutchinson, G. Kantor, W. Burgardand L. Kavraki, and Sebastian Thrun. *Principles of Robot Motion: Theory, Algorithms and Implementations*. MIT Press, 2005.

[7] Lars B. Cremean, Tully B. Foote, Jeremy H. Gillula, George H. Hines, Dmitriy Kogan, Kristopher L. Kriechbaum, Jeffrey C. Lamb, Jeremy Leibs, Laura Lindzey, Christopher E. Rasmussen, Alexander D. Stewart, Joel W. Burdick, and Richard M. Murray. Alice: An information-rich autonomous vehicle for high-speed desert navigation. *Journal of Field Robotics*, 23(9):777–810, 2006.

[8] Carl de Boor. *A Practical Guide to Splines*. Springer Verlag, New York, 1978.

[9] Ronald De Vore, Guergana Petrova, and Vladimir Temlyakov. Best basis selection for approximation in L_p. *Found. Comput. Math.*, 3(2):161–185, 2003.

[10] Ronaldo Dias. Density estimation via hybrid splines. *Journal of Statistical Computation and Simulation*, 60:277–294, 1998.

[11] Ronaldo Dias. Sequential adaptive non parametric regression via H-splines. *Communications in Statistics: Computations and Simulations*, 28:501–515, 1999.

[12] Ronaldo Dias. A note on density estimation using a proxy of the Kullback-Leibler distance. *Brazilian Journal of Probability and Statistics*, 13(2):181–192, 2000.

[13] Jean-Paul Laumond editor, editor. *Robot Motion Planning and Control*, volume 229 of *Lecture Notes in Control and Information Science*. Springer, Berlin, 1998. Available online:http://www.laas.fr/ jpl/book.html.

[14] Don Grundel, Robert Murphey, Panos Pardalos, and Oleg Prokopyev, editors. *Cooperative systems, Control and Optimization*, volume 588 of *Lecture Notes in Economics and Mathematical Systems*. Springer, Berlin, 2007.

[15] Michael J. Hirsch, Panos Pardalos, Robert Murphey, and Don Grundel, editors. *Advances in cooperative control and optimization*, volume 369 of *Lecture Notes in Control and Information Sciences*. Springer, Berlin, 2008. Papers from a meeting held in Gainesville FL, January 31– February 2, 2007.

[16] Yussef Jabri. *The Mountain Pass Theorem: Variants, Generalizations and Some Applications*. Cambridge University Press, 2003.

[17] Robert Kohn, J. S. Marron, and Paul Yau. Wavelet estimation using Bayesian basis selection and basis averaging. *Statist. Sinica*, 10(1):109–128, 2000.

[18] Charles Kooperberg and Charles J. Stone. A study of logspline density estimation. *Computational Statistics and Data Analyis*, 12:327–347, 1991.

[19] S. Lavalle. *Planning Algorithms.* Cambridge University Press, 2006.

[20] Zhen Luo and Grace Wahba. Hybrid adaptive splines. *Journal of the American Statistical Association*, 92:107–116, 1997.

[21] Ulrich Reif. Orthogonality of cardinal B-splines in weighted Sobolev spaces. *SIAM J. Math. Anal.*, 28(5):1258–1263, 1997.

[22] B. W. Silverman. *Density Estimation for Statistics and Data Analysis.* Chapman and Hall (London), 1986.

[23] Abhishek Tiwari, Harish Chandra, Jacob Yadegar, and Junxian Wang. Constructing optimal cyclic tours for planar exploration and obstacle avoidance: A graph theory approach. In *Advances in Variable Structure And Sliding Mode Control*. Springer, 2007.

[24] Brani Vidakovic. *Statistical modeling by wavelets.* Wiley Series in Probability and Statistics: Applied Probability and Statistics. John Wiley & Sons Inc., New York, 1999. A Wiley-Interscience Publication.